Pole Identification for The Universal Line Model Based on Trace Fitting

Bjørn Gustavsen, *Senior Member, IEEE*, and John Nordstrom

***Abstract*—The universal line model (ULM) is a frequency dependent transmission-line model based on the method of characteristics in the phase domain. Although the ULM is known to produce highly accurate models for both overhead lines and underground cables, situations have been encountered where the pole identification for the propagation function fails. In this paper, we overcome the problem by basing the pole identification on trace fitting rather than mode fitting. This is achieved by introducing delayed basis functions in the vector fitting algorithm, followed by time-delay refinement and model-order reduction. In situations where the modes can be fitted without difficulty, the existing approach using modes obtained by a frequency-dependent transformation matrix remains the most accurate.**

***Index Terms*—Electromagnetic transients, frequency dependency, transmission-line model, universal line model (ULM), vector fitting.**

NOMENCLATURE

Bold, capital letter $(\mathbf{Y})$	Matrix of elements.
Bold, small letter $(\mathbf{y})$	Vector of elements.
Small letter (y)	Single element.

I. INTRODUCTION

THE accurate simulation of electromagnetic transients in power systems requires that overhead line and underground cable models include all frequency-dependent effects. This has traditionally been accomplished using formulations based on a constant transformation matrix and frequency-dependent modes [1], [2]. Approximation of the modes with rational functions and a single time delay leads to recursive convolutions in the time domain and, thus, highly efficient simulations [1]. The frequency dependency of the transformation matrix can be taken into account by an additional convolution [3], [4], but this works well only for underground cables (as unstable poles may be needed when applied to overhead lines). This has led to the development of a new class of models where the fitting is accomplished directly in phase coordinates, either via fitting in the z-domain [5], [6] or the s-domain [7]–[11].

One of the phase-domain models—the universal line model (ULM) [10], [11]—has been available in two electromagnetic-transient (EMT) programs since 1998 and 2001, respectively. This model has proven to be highly accurate for both overhead lines and underground cables. The key idea is to first decompose the propagation function into modes, each fitted with a set of poles and a single time delay, followed by a final fitting in the phase domain with only residues as unknown quantities. By increasing the fitting order, a model of arbitrary accuracy can be obtained.

A case where the pole-identification procedure is unable to obtain a high-quality model is reported, for the first time, in this paper. In order to overcome this deficiency, we propose an alternative pole-identification procedure that relies on fitting the matrix trace rather than the modes. The main contribution is the implementation of the trace fitting procedure, which requires the inclusion of multiple time delays in the fitting process. This is achieved by introducing delayed basis functions in the pole-relocating, vector-fitting (VF) algorithm [12], followed by time-delay refinement. Finally, a model-order reduction (MOR) approach proposed in [18] is used to reduce the model size. The performance of the new pole-identification scheme is demonstrated by an application to two different cable systems.

II. UNIVERSAL LINE MODEL

A. Method of Characteristics in the Phase Domain

Consider a transmission line with ends denoted k and m, respectively. The relationship between voltage $\mathbf{v}$ and current $\mathbf{i}$ at line end k in the frequency domain is given by

$$\mathbf{i}_k = \mathbf{Y}_c \mathbf{v}_k - 2\mathbf{i}_{ki} \tag{1}$$

$$\mathbf{i}_{ki} = \mathbf{H}^T \mathbf{i}_{mr} \tag{2}$$

where indices i and r denote the incident and reflected waves, respectively. The matrices for surge admittance $\mathbf{Y}_c$ and propagation function $\mathbf{H}$ for a line of length l are obtained from the series impedance matrix $\mathbf{Z} = \mathbf{R} + s\mathbf{L}$ and the shunt admittance matrix $\mathbf{Y} = \mathbf{G} + s\mathbf{C}$ as

$$\mathbf{Y}_c = \mathbf{Z}^{-1}\sqrt{\mathbf{ZY}} \tag{3}$$

$$\mathbf{H} = e^{-\sqrt{\mathbf{ZY}}l}. \tag{4}$$

B. Rational Fitting

In the universal line model (ULM), the poles $\{a_m\}$ for $\mathbf{Y}_c$ are obtained by fitting the matrix trace (5) [11] using VF, followed

Manuscript received December 6, 2006; revised February 14, 2007. This work was supported in part by the Norwegian Research Council, in part by Aker Kvaerner, in part by Compagnie Deutsch, in part by FMC Technologies, in part by FRAMO, in part by Norsk Hydro, in part by Petrobras, in part by Siemens, in part by Statoil, in part by Total, and by Vetco Gray. Paper no. TPWRD-00783-2006.

B. Gustavsen is with SINTEF Energy Research, Trondheim N-7465, Norway (e-mail: bjorn.gustavsen@sintef.no).

J. Nordstrom is with the Manitoba HVDC Research Centre Inc., Winnipeg, MB R3J 3W1 Canada (e-mail: johnn@hvdc.ca).

Digital Object Identifier 10.1109/TPWRD.2007.911186

by a final fitting of the residues $\mathbf{R}_m$ and proportional term $\mathbf{D}$ in the phase domain (6)

$$tr(\mathbf{Y}_c) \cong \sum_{m=1}^{N} \frac{r_m}{s - a_m} + d \tag{5}$$

$$\mathbf{Y}_c \cong \sum_{m=1}^{N} \frac{\mathbf{R}_m}{s - a_m} + \mathbf{D}. \tag{6}$$

It is also remarked that the fitting can be achieved by applying VF to the columns of $\mathbf{Y}_c$ [8], [10], providing a private pole set for each column; the latter gives a more accurate result with a given order. However, since PSCAD makes use of a nonsparse, Fortran 77 implementation of VF with fixed array dimensions, it was decided to calculate the poles by trace fitting in order to minimize memory requirements. Trace fitting has also been applied to network equivalent modeling [13].

Poles $\{a_m\}$ and delays τ for the fitting of $\mathbf{H}$ are obtained by fitting the modes h_i of $\mathbf{H}$

$$h_i \cong \sum_{m=1}^{N_i} \frac{r_m}{s - a_{m,i}} e^{-s\tau_i}, \quad i = 1, \ldots, n. \tag{7}$$

Modes with nearly equal delays are lumped together before the fitting is performed. Finally, the residues $\{\mathbf{R}_m\}$ are calculated by solving (7) with (known) poles and delays

$$\mathbf{H} \cong \sum_{g=1}^{G} \left(\sum_{m=1}^{N_g} \frac{\mathbf{R}_{m,g}}{s - a_{m,g}} \right) e^{-s\tau_g}. \tag{8}$$

In (8), G denotes the number of (lumped) modes and N_g is the number of poles used for fitting the gth mode.

III. Accuracy Problem

In the original ULM formulation [10], the modes of $\mathbf{H}$ are obtained via a constant, real transformation matrix. This transformation matrix is evaluated at the highest frequency point s_n in the band of interest

$$\mathbf{T}_n^{-1} \mathbf{Z} \mathbf{Y} \mathbf{T}_n = \mathrm{diag}(\boldsymbol{\lambda}). \tag{9}$$

The columns of (the complex) $\mathbf{T}_n$ are rotated to minimize the imaginary part in the least-squares sense and the imaginary parts are discarded. The resulting transformation matrix $\mathbf{T}_0$ is applied to $\mathbf{ZY}$ (9) at all frequencies and the offdiagonal elements are discarded. From each modal component $\lambda(s)$, the associated propagation component is calculated as

$$h(s) = e^{-\sqrt{\lambda(s)}l}. \tag{10}$$

As the diagonalization by (10) may cause the (diagonal) elements to contain contributions from more than a single mode, one would expect that obtaining the modes directly from (9) with a frequency dependent, complex $\mathbf{T}$, would lead to a more accurate result for (8). Calculated results have verified this assertion for several cases, and use of a frequency dependent $\mathbf{T}$ was, as a consequence, applied to the ULM implementation in PSCAD [11]. Smooth modes resulted when artificial eigenvector switchovers were removed; this was achieved by resorting to a Newton diagonalization technique, which uses the modal decomposition at a given frequency sample as the initial value for the next frequency sample [14].

Some situations have been encountered where the modes cannot be decently fitted, whether they are obtained by a constant or a frequency dependent $\mathbf{T}$. This difficulty can be explained as follows.

1) With a constant $\mathbf{T}$, the modes are linear combinations of the elements of $\mathbf{H}$ with constant, real coefficients. Since the diagonalization is not complete over the full frequency band, each mode will be composed of a dominant component plus "parasitic" components with different delays. This is shown in (11) for a two-conductor line. When fitting this contaminated mode with a rational function plus a single delay, the extracted poles are affected by the delay factor of the parasitic component. In order words, incorrect poles result due to an incorrect model structure

$$h_1(s)e^{-s\tau_1} + \Delta h_2(s)e^{-s\tau_2} \cong h_{rat}(s)e^{-s\tau}. \tag{11}$$

2) With a frequency dependent $\mathbf{T}$, the modes are linear combinations of the elements of $\mathbf{H}$ with frequency dependent, complex coefficients. This frequency dependency causes the poles of the modes to become different from those of $\mathbf{H}$. This is demonstrated in the Appendix for a lumped circuit.

IV. Pole Identification Based on Trace Fitting

A. Trace Fitting

In order to overcome the difficulties with mode fitting, fitting the trace of $\mathbf{H}$, as is similarly done for $\mathbf{Y}_c$ in (5), is proposed. The trace (12) captures all of the essential information of $\mathbf{H}$ since it is equal to the sum of the eigenvalues of $\mathbf{H}$, λ_i [15]. At the same time, $tr(\mathbf{H})$ is equal to the sum of the diagonal elements and thereby it contains the poles of $\mathbf{H}$

$$tr\left(\mathbf{H}(s)\right) = \sum_i \lambda_i(s) = \sum_i \mathbf{H}_{ii}(s). \tag{12}$$

The problem to be solved is

$$tr\left(\mathbf{H}(s)\right) \cong \sum_{g=1}^{G} \left(\sum_{m=1}^{N_g} \frac{r_{m,g}}{s - a_{m,g}} e^{-s\tau_g} \right). \tag{13}$$

Solving (13) requires identification of all poles and delays simultaneously. Currently, no approach exists that can achieve this in an efficient and reliable manner; we overcome this difficulty by identifying a common pole set for all delay groups

$$tr\left(\mathbf{H}(s)\right) \cong \sum_{g=1}^{G} \left(\sum_{m=1}^{N} \frac{r_m}{s - a_m} e^{-s\tau_g} \right). \tag{14}$$

The time delays are first extracted by fitting the modes obtained by a real transformation matrix (10), using the "optimal" delay extraction procedure in [16]. The poles in (14) are subsequently identified by a modified version of VF that uses delayed

```
for n=1:N_G
  rmserr_0 = fit(poles,tau_n)
  for iter=1:Niter
    tau_n = tau_n +Δ
    rmserr = fit(poles,tau_n)
    if rmserr > rmserr_0
      Δ=−Δ/2
    end
    rmserr_0=rmserr
  end
end
```

Fig. 1. Pseudocode for inclusion of delays in the optimization.

basis functions. With the relaxed normalization in [17], we obtain the following linear LS problem for the pole-identification step:

$$\left(\sum_{m=1}^{N}\frac{\tilde{r}_m}{s-a_m}+\tilde{d}\right)tr\left(\mathbf{H}(s)\right)\cong\sum_{g=1}^{G}\left(\sum_{m=1}^{N}\frac{r_{m,g}}{s-a_m}e^{-s\tau_g}\right). \tag{15}$$

After solving (15), new poles are calculated as

$$\{a_m\}=\mathrm{eig}(\mathbf{A}-\mathbf{b}\tilde{d}^{-1}\tilde{\mathbf{r}}^T) \tag{16}$$

where $\mathbf{b}$ is a column of one's and $\tilde{r}^T$ is a row-vector holding the residues $\{\tilde{r}_m\}$. This procedure relocates a set of initial poles to their final positions by repeated usage of (15) and (16). Finally, the unknown residues for (14) are calculated with known poles and delays.

B. Time-Delay Refinement

The accuracy of the fitting (14) can be improved by an iterative refinement to the time delays. A simple search procedure is used that optimizes the time delays one-by-one, so as to minimize the rms error in (14) (an overview of the procedure is shown in Fig. 1). The delay is increased incrementally until the rms error starts to increase. The step length is then reduced by half and the search direction is reversed. Unnecessary evaluations are avoided by storing the rms error versus delay in tables. More advanced search routines, such as Brent's method, can also be used, see [16]. Since the delays are refined one-by-one, it may be necessary to repeat the refinement process a few times (we used three repetitions in this work).

C. Model-Order Reduction

The use of identical poles for all modes makes the fitting process more constrained, thus requiring a higher fitting order compared to the usage of a private pole set for each mode. To alleviate this problem, we first calculate a high-order common pole set fitting, from which we select a subset of poles.

Equation (14) leads to a linear problem of the form (17) where each frequency sample, k gives one row (18)

$$\mathbf{A}\mathbf{x}=\mathbf{b} \tag{17}$$

$$A_k=\left[\frac{e^{-s_k\tau_1}}{s_k-a_1}\quad\cdots\quad\frac{e^{-s_k\tau_1}}{s_k-a_N}\quad\cdots\quad\frac{e^{-s_k\tau_G}}{s_k-a_1}\quad\cdots\quad\frac{e^{-s_k\tau_G}}{s_k-a_N}\right]. \tag{18}$$

In the case of complex poles, the basis functions (columns of $\mathbf{A}$) that are associated with a complex conjugate pair $\{a_m,a_{m+1}\}$ are replaced with

$$\varphi_m=\frac{e^{-s\tau_i}}{s-a_m}+\frac{e^{-s\tau_i}}{s-a_m^*},\quad\varphi_{m+1}=\frac{je^{-s\tau_i}}{s-a_m}-\frac{je^{-s\tau_i}}{s-a_m^*}. \tag{19}$$

This causes the associated elements in $\mathbf{x}$ to be real only, which are $\mathrm{Re}\{r_m\}$ and $\mathrm{Im}\{r_m\}$, respectively [12]. Finally, the problem (17) is converted to real only

$$\mathbf{A}'\mathbf{x}=\mathbf{b}',\quad\mathbf{A}'=\begin{bmatrix}\mathrm{Re}\{\mathbf{A}\}\\ \mathrm{Im}\{\mathbf{A}\}\end{bmatrix},\quad\mathbf{b}'=\begin{bmatrix}\mathrm{Re}\{\mathbf{b}\}\\ \mathrm{Im}\{\mathbf{b}\}\end{bmatrix}. \tag{20}$$

The conditioning of $\mathbf{A}'$ is improved by scaling its columns to unit length

$$\mathbf{A}'_{col}:=\frac{\mathbf{A}'_{col}}{q_{col}} \tag{21}$$

where

$$q_{col}=\|\mathbf{A}'_{col}\|_2\,. \tag{22}$$

MOR is applied to (20), based on the approach in [18]. For the (scaled) system-matrix $\mathbf{A}'$, the singular value decomposition is computed

$$\mathbf{A}'=\mathbf{U}\mathbf{S}\mathbf{V}^T. \tag{23}$$

By replacing singular values $\mathbf{S}_{ii}$ in (23) that are smaller than a threshold value $\mathbf{S}_{11}\cdot tol$ with zero, a modified system matrix $\mathbf{A}''$ is obtained. The problem $\mathbf{A}''\mathbf{x}=\mathbf{b}'$ is solved using the backslash operator "\" in Matlab, which invokes QR decomposition with rank revealing column pivoting [19]. This procedure causes $\mathbf{x}$ to possess as many zeros as $\mathbf{A}''$ has zero singular values. The nonzero elements of $\mathbf{x}$ define the subset of poles to be retained.

The solution vector is finally scaled back to recover the final result

$$\mathbf{x}_{col}:=\frac{\mathbf{x}_{col}}{q_{col}}. \tag{24}$$

V. Example: Armored Single-Core Cables

A. Cable Geometry

Fig. 2 shows an example of three, armored single-core cables. Each cable features two metallic sheaths and one layer of metallic armor. The armor is eliminated from the system of conductors, leading to a nine-conductor system. Details about the cable geometry are given in Table I.

B. Mode Fitting

The nine modes of propagation were calculated in the frequency range of 1 Hz–1 MHz using a frequency dependent, complex $\mathbf{T}$. It can be seen from the modal velocities in Fig. 3 that there are only three distinct modes at high frequencies. The modes were lumped accordingly into three modes, and then subjected to rational fitting (7) with refinement of time delays [16].

Fig. 4 shows the fitted modes when using 14 stable poles per mode. The fitting error is seen to be large for two of the modes as the mode fitting approach breaks down. The problem occurs

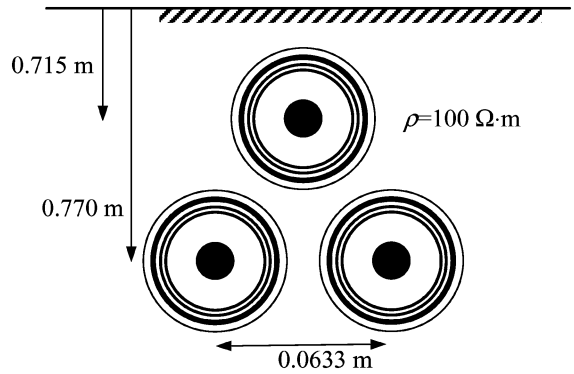

Fig. 2. Three armored cables. Length: 24 km.

TABLE I
CABLE DATA

Item	Property
Copper core	OD=18.3 mm , ρ= 1.69*E*–8 Ω·m
Insulation	*t*=9.88 mm, ε_r=3.2
Core screen	t=0.06 mm , ρ= 1.69*E*–8 Ω·m
Insulation	*t*=1.3 mm, ε_r=2.8
Teredo barrier	*t*=0.1 mm, ρ= 6.4*E*–8 Ω·m
Insulation	*t*=3.26 mm ε_r=1.0
Armor	*t*=2.5 mm , ρ= 3.6*E*–8 Ω·m
Insulation	*t*=5 mm, ε_r=2.25

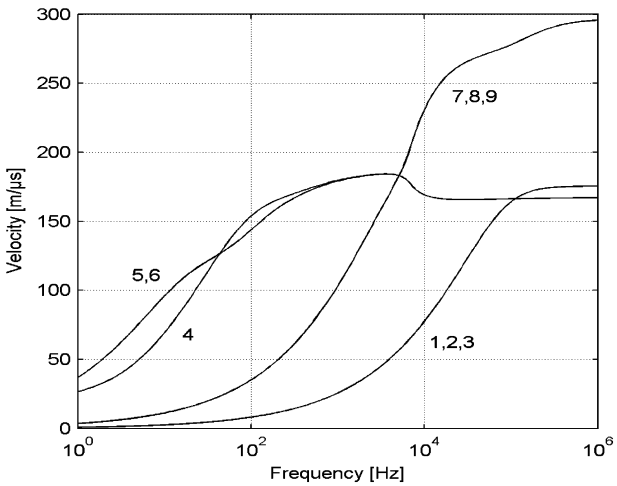

Fig. 3. Modal velocities.

because the modes require unstable poles to be accurately fitted.

Fig. 5 shows the same result when the modes are obtained using a constant, real $\mathbf{T}$ calculated at 1 MHz. The modes are now all fitted with a high degree of accuracy.

The poles and delays obtained (via a constant $\mathbf{T}$) were used as known quantities for the final fitting of $\mathbf{H}$. The result in Fig. 6 shows that the deviation curves peak at more than $1E-2$ around 100 kHz, which is a much higher error level than that of the modes (Fig. 5). A somewhat more accurate result was obtained when using poles and delays obtained via a frequency dependent $\mathbf{T}$, despite the very poor fitting of the modes (Fig. 4).

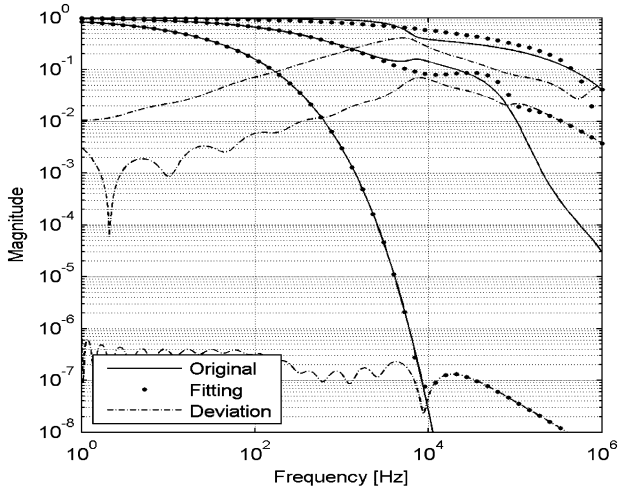

Fig. 4. Modes of $\mathbf{H}$ obtained via frequency dependent, complex $\mathbf{T}$.

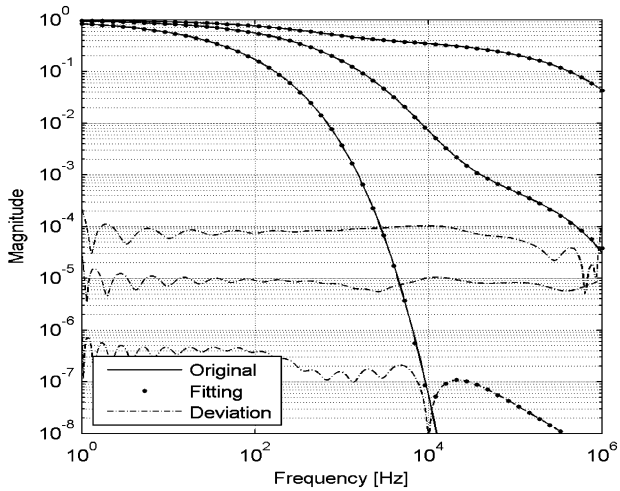

Fig. 5. Modes of $\mathbf{H}$ obtained via constant, real $\mathbf{T}$.

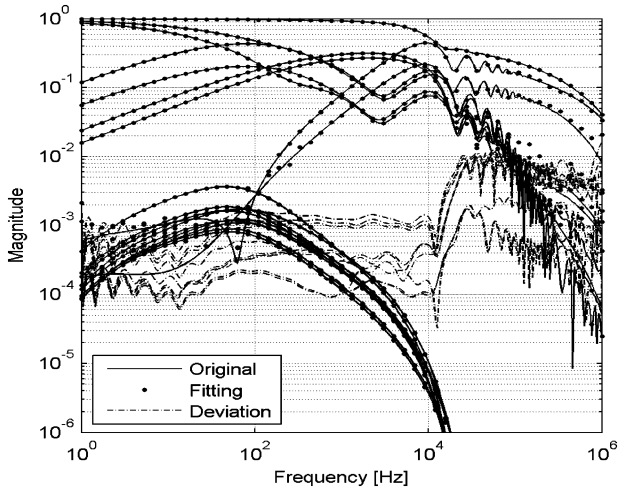

Fig. 6. Fitted $\mathbf{H}$.

C. Trace Fitting

Initial time delays were obtained by mode fitting via a constant $\mathbf{T}$, using 40 poles per delay group. This gave a fit with an

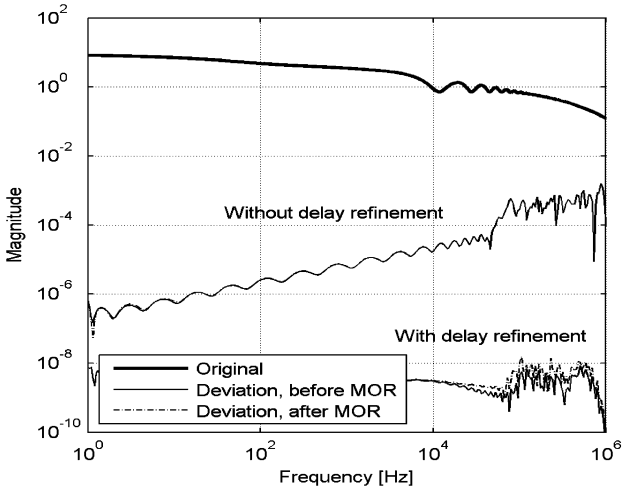

Fig. 7. Fitted trace.

TABLE II
MODAL DELAYS [μS]

Before delay refinement	79.0	143.3	196.9
After delay refinement	78.9	141.2	196.5

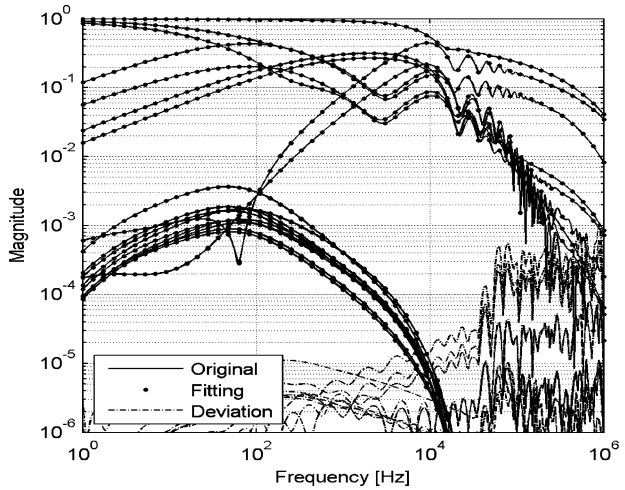

Fig. 8. Fitted $\mathbf{H}$, without delay refinement, after MOR.

rms error smaller than $1E-7$, for all modes. With these delays as known quantities, trace fitting was applied using 40 poles per delay group, with iterative delay refinement and MOR, and discarding singular values smaller than $tol = 1E-14$. Use of MOR resulted in the order being reduced from $3 \times 40 = 120$ to 88 poles. Fig. 7 shows the fitting result for the trace. It is seen that delay refinement greatly improves the accuracy, and that the impact of MOR on accuracy is insignificant. The change to the delays is shown in Table II.

Figs. 8 and 9 show the final fitting for $\mathbf{H}$, without and with delay refinement, respectively—again, delay refinement leads to a great improvement in accuracy. From this result, one can conclude that the delays obtained from mode fitting are not optimal with respect to the final fitting of $\mathbf{H}$.

Fig. 10 compares the fitting accuracy for $\mathbf{H}$ in terms of rms error, for different approaches and fitting orders. The lumped

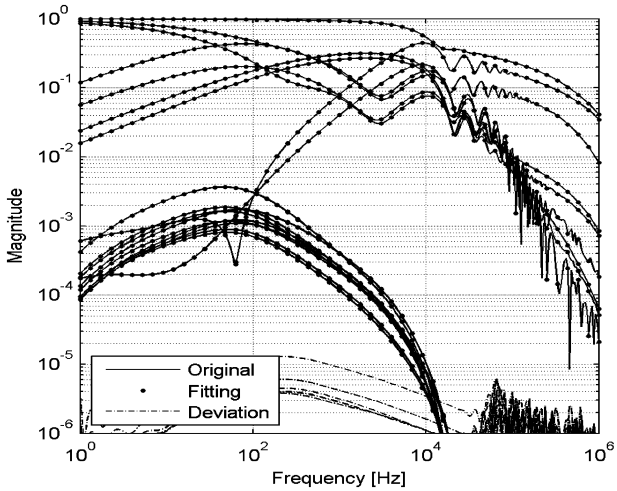

Fig. 9. Fitted $\mathbf{H}$, with delay refinement, after MOR.

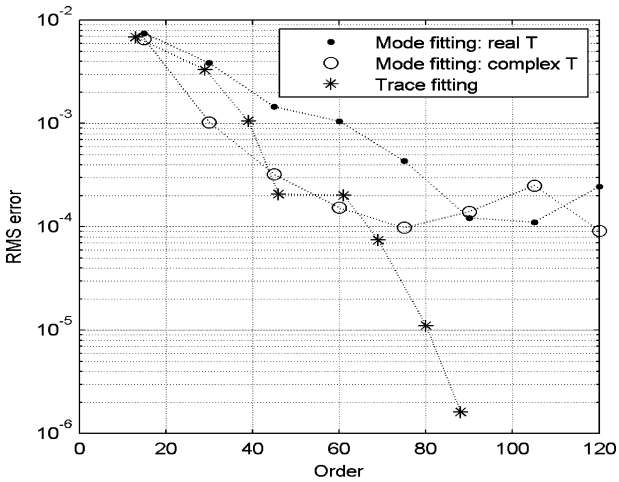

Fig. 10. RMS error versus fitting order.

modes were each fitted using orders 5, 10,. . ., 40 poles. Since there are three (lumped) modes, the order with mode fitting is three times these values, as can be observed in Fig. 10. The trace is fitted using the same orders, followed by MOR. It can be seen that the usage of trace fitting yields highly accurate results for sufficiently high orders, while mode fitting is not capable of producing rms errors smaller than $1E-4$. The result is particularly bad when using a constant, real $\mathbf{T}$.

D. Time-Domain Results

The obtained rational model via trace fitting is fully compatible with the time-domain ULM implementation in PSCAD. In Fig. 11, an example where the cable system is subjected to a step voltage excitation on a core conductor is shown. The far-end voltage (V_{10}) on the same core conductor is to be calculated.

The trace was fitted using $3 \times 25 = 75$ poles followed by order reduction. This resulted in a model with a total of 69 poles, along with an rms error of about $7E-5$, see Fig. 10. For validation purposes, the transfer function V_{10}/V_1 was calculated in the frequency domain via the exact PI equivalent of the cable. A highly

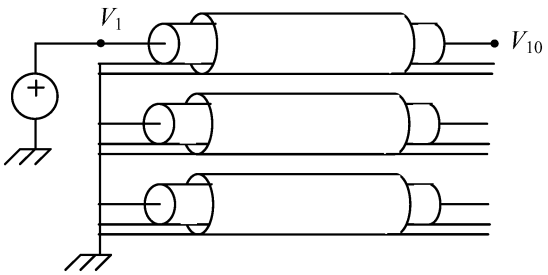

Fig. 11. Step voltage excitation.

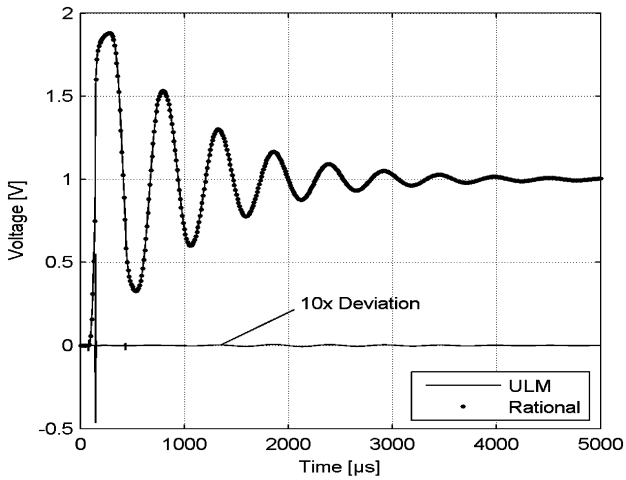

Fig. 12. PSCAD simulation of step response.

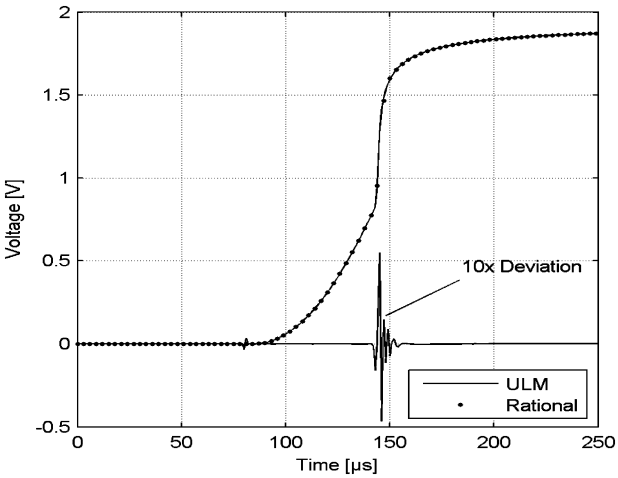

Fig. 13. PSCAD simulation of step response. Expanded view.

accurate, rational fitting of this frequency response was calculated by VF, and the rational model was included in PSCAD by convolution with a user-written subroutine [20].

Fig. 12 compares the simulated step voltage response by the ULM and by the rational model. In addition, the deviation by the two responses, multiplied by a factor of 10, is shown. The deviation is very small, except for a high-frequency transient (>1 MHz), which results because the rational model is fitted only up to 1 MHz, leading to a Gibbs type of oscillation in the response, see Fig. 13.

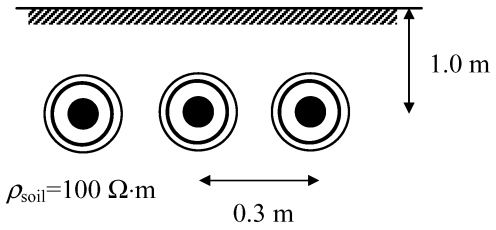

Fig. 14. Cable configuration. Cable length: 10 km.

TABLE III
CABLE DATA

Item	Property
Core	OD=39 mm , ρ= 3.365E–8 Ω·m
Insulation	t=18.25 mm, ε_r=2.85
Sheath	t=0.22 mm , ρ= 1.718E–8 Ω·m
Jacket	t=4.53 mm, ε_r=2.51

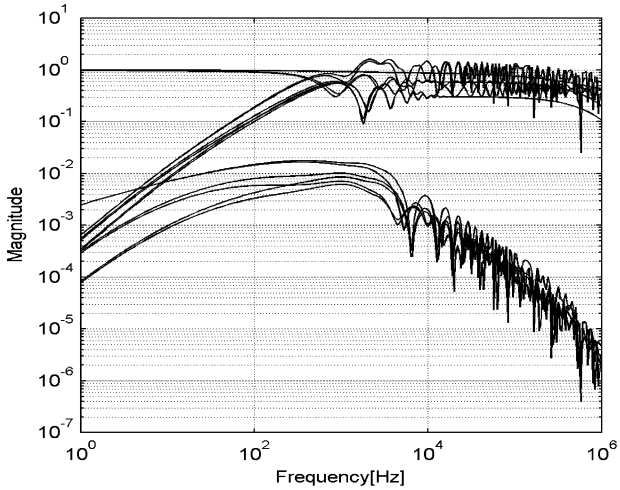

Fig. 15. Propagation function $\mathbf{H}$.

VI. EXAMPLE: SINGLE-CORE COAXIAL CABLES

The current version of the ULM, as implemented in EMTP-type programs, has, in general, been highly successful, where fitting problems such as that reported in Section V are more of an exception. It is therefore useful to investigate the performance of the trace fitting approach when applied to more typical examples.

Fig. 14 shows a system of three, 145-kV single-core coaxial cables (see data in Table III). The propagation function for this six-conductor line is shown in Fig. 15. For such cable systems, it is sometimes necessary to obtain a very accurate fit in order to simulate the induced sheath overvoltages (small elements in Fig. 15). This may require deviation levels smaller than $1E-4$.

The six modes were lumped into four modes, which were each subjected to rational fitting for delay identification, where the same fitting order was used for all four modes. Fig. 16 shows the rms error for the fitted results of $\mathbf{H}(s)$, when using either the trace fitting approach or the existing mode fitting techniques. The results are shown for different orders when fitting the modes: 5, 10,. . ., 20. It can be seen that with mode fitting, using a frequency-dependent complex $\mathbf{T}$ leads to a substantially better result than with the use of a constant, real

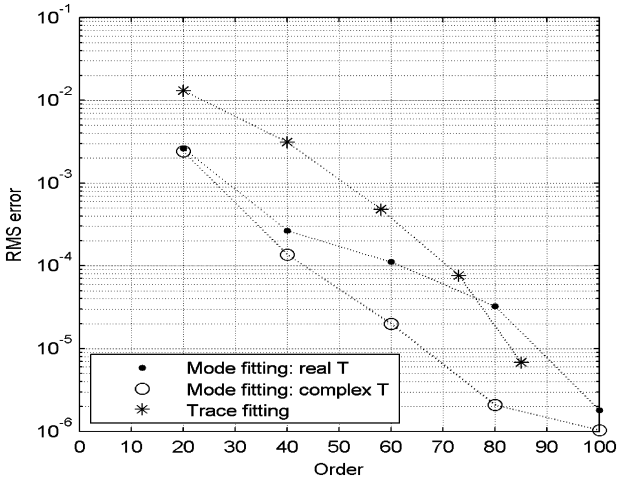

Fig. 16. RMS error versus fitting order.

$\mathbf{T}$. (This was also the reason for introducing the complex $\mathbf{T}$ [11]). Using trace fitting provides substantially higher rms error for a given order. For instance, a 72nd-order approximation is needed for an error level of $1E-4$, while only a 40th-order fitting is needed with modal fitting and a complex $\mathbf{T}$.

VII. Discussion

The trace fitting approach is applicable to any overhead line and underground cable, since it does not require that the modes of $\mathbf{H}$ be fitted (thereby avoiding the problem of nonfittable modes and mixed modes). On the other hand, trace fitting leads, in most situations, to a less accurate result than mode fitting, and should therefore only be used when mode fitting fails. The decreased accuracy with trace fitting is not an intrinsic property, but rather a consequence of the implemented fitting approach. Delayed basis functions (partial fractions) are introduced in VF, leading to fitting with a common pole set for all of the delay groups. A more accurate result would be achieved if it was possible to conduct the fitting using a private pole set for each delay group. This was partly achieved in this work using "overfitting," followed by MOR. This approach obtains a private pole set for the delay groups by picking a subset of the poles. However, a direct computation of the private pole sets would lead to a more accurate result.

In the example in Section VI with three SC cables, mode fitting gave a substantially more accurate result for the fitting of $\mathbf{H}$ than trace fitting. In this case, the delay refinement in the trace fitting approach barely changed the delays at all. On the other hand, in the example in Section V with three armored cables, the delay refinement greatly improved the accuracy, which led the trace fitting approach to give a more accurate fit for $\mathbf{H}$. Thus, the use of mode fitting does not guarantee the production of the most suitable time delays for the fitting of $\mathbf{H}$.

VIII. Conclusion

1) The existing version of the ULM identifies the poles of the propagation function via mode fitting, using either a constant or a frequency-dependent transformation matrix. Certain cable systems exist where these approaches fail.

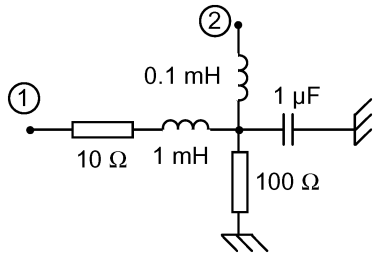

Fig. 17. Two-port network.

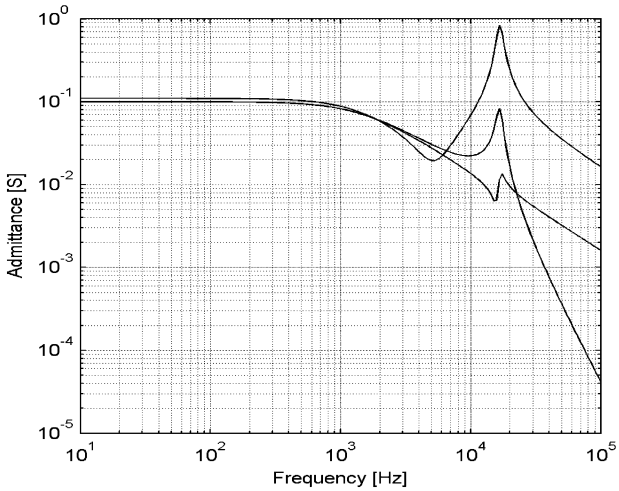

Fig. 18. Elements of $\mathbf{Y}$.

2) Pole identification via trace fitting is introduced as an alternative approach. The trace fitting is achieved by introducing delayed basis functions in the vector fitting algorithm, followed by delay refinement and MOR. This approach is shown to work well in an example where mode fitting fails to give an acceptable result.
3) Trace fitting should not replace mode fitting as the default approach, since mode fitting using a frequency dependent, complex transformation matrix will, in most situations, lead to a more accurate model.

Appendix
Pole Identification

The following demonstrates that modes obtained via a frequency-dependent transformation matrix $\mathbf{T}$ will not necessarily produce the correct poles. This example consists of the terminal admittance $\mathbf{Y}$ of a two-port network (see Fig. 17). The frequency behavior of $\mathbf{Y}$ is shown in Fig. 18. The poles are identified by VF using the following approaches:

1) fitting all matrix elements of $\mathbf{Y}$ simultaneously;
2) fitting matrix trace;
3) fitting modes obtained by a real $\mathbf{T}$, calculated at 1 kHz;
4) fitting modes obtained by a frequency dependent $\mathbf{T}$.

Fig. 19 shows the rms error for the final fitting of $\mathbf{Y}$ with a pole-residue model of the form (6). It can be seen that the first three approaches allow $\mathbf{Y}$ to be fitted to machine precision, by using only three poles. With mode fitting and a frequency dependent $\mathbf{T}$, a slightly different pole set is extracted, and so, a less accurate fitting of $\mathbf{Y}$ results. It is remarked that the nature of

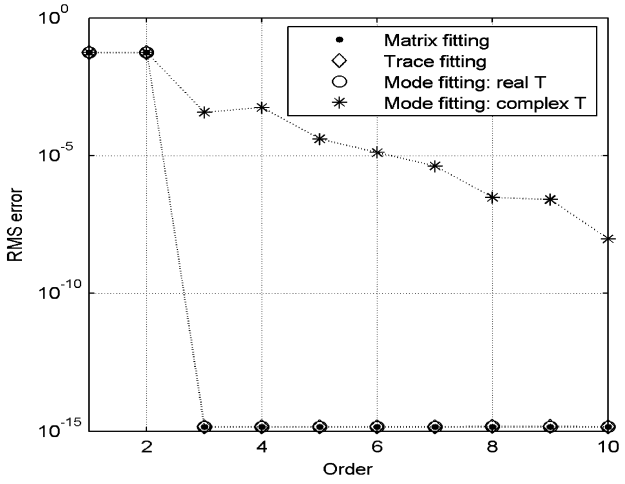

Fig. 19. RMS error of fitted $\mathbf{Y}$.

the fitting problem is different from that reported for the cable system. In the latter case, a very accurate fit could be obtained if unstable poles were allowed, whereas the use of unstable poles does not improve the result in Fig. 19.

REFERENCES

[1] A. Semlyen and A. Dabuleanu, "Fast and accurate switching transient calculations on transmission lines with ground return using recursive convolutions," *IEEE Trans. Power App. Syst.*, vol. PAS-94, no. 2, pt. 1, pp. 561–575, Mar./Apr. 1975.

[2] J. R. Marti, "Accurate modelling of frequency-dependent transmission lines in electromagnetic transient simulations," *IEEE Trans. Power App. Syst.*, vol. PAS-101, no. 1, pp. 147–157, Jan. 1982.

[3] L. Marti, "Simulation of transients in underground cables with frequency-dependent modal transformation matrices," *IEEE Trans. Power Del.*, vol. 3, no. 3, pp. 1099–1110, Jul. 1988.

[4] B. Gustavsen and A. Semlyen, "Simulation of transmission line transients using vector fitting and modal decomposition," *IEEE Trans. Power Del.*, vol. 13, no. 2, pp. 605–614, Apr. 1998.

[5] G. Angelidis and A. Semlyen, "Direct phase-domain calculation of transmission line transients using two-sided recursions," *IEEE Trans. Power Del.*, vol. 10, no. 2, pp. 941–949, Apr. 1995.

[6] T. Noda, N. Nagaoka, and A. Ametani, "Phase domain modeling of frequency-dependent transmission lines by means of an ARMA model," *IEEE Trans. Power Del.*, vol. 11, no. 1, pp. 401–411, Jan. 1996.

[7] H. V. Nguyen, H. W. Dommel, and J. R. Marti, "Direct phase-domain modelling of frequency-dependent overhead transmission lines," *IEEE Trans. Power Del.*, vol. 12, no. 3, pp. 1335–1342, Jul. 1997.

[8] B. Gustavsen and A. Semlyen, "Combined phase and modal domain calculation of transmission line transients based on vector fitting," *IEEE Trans. Power Del.*, vol. 13, no. 2, pp. 596–604, Apr. 1998.

[9] B. Gustavsen and A. Semlyen, "Calculation of transmission line transients using polar decomposition," *IEEE Trans. Power Del.*, vol. 13, no. 3, pp. 855–862, Jul. 1998.

[10] A. Morched, B. Gustavsen, and M. Tartibi, "A universal model for accurate calculation of electromagnetic transients on overhead lines and underground cables," *IEEE Trans. Power Del.*, vol. 14, no. 3, pp. 1032–1038, Jul. 1999.

[11] B. Gustavsen, G. Irwin, R. Mangelrød, D. Brandt, and K. Kent, "Transmission line models for the simulation of interaction phenomena between parallel AC and DC overhead lines," in *Proc. Int. Conf. Power System Transients*, Jun. 20–24, 1999, pp. 61–67.

[12] B. Gustavsen and A. Semlyen, "Rational approximation of frequency domain responses by vector fitting," *IEEE Trans. Power Del.*, vol. 14, no. 3, pp. 1052–1061, Jul. 1999.

[13] T. Noda, "Identification of a multiphase network equivalent for electromagnetic transient calculations using partitioned frequency response," *IEEE Trans. Power Del.*, vol. 20, no. 2, pt. 1, pp. 1134–1142, Apr. 2005.

[14] L. M. Wedepohl, H. V. Nguyen, and G. D. Irwin, "Frequency-dependent transformation matrices for untransposed transmission lines using Newton-Raphson method," *IEEE Trans. Power Syst.*, vol. 11, no. 3, pp. 1538–1546, Aug. 1996.

[15] L. N. Trefethen and D. Bau, *Numerical Linear Algebra*. Philadelphia, PA: SIAM, 1997, p. 186, 0-89871-361-7.

[16] B. Gustavsen, "Time delay identification for transmission line modeling," in *Proc. 8th IEEE Workshop Signal Propagation Interconnects*, Heidelber, Germany, May 9–12, 2004, pp. 103–106.

[17] B. Gustavsen, "Improving the pole relocating properties of vector fitting," *IEEE Trans. Power Del.*, vol. 21, no. 3, pp. 1587–1592, Jul. 2006.

[18] A. Ramirez, A. Semlyen, and R. Iravani, "Order reduction of the dynamic model of a linear weakly periodic system—Part I: General methodology," *IEEE Trans. Power Syst.*, vol. 19, no. 2, pp. 857–865, May 2004.

[19] Å. Bjørck, *Numerical Methods for Least Squares Problems*. Philadelphia, PA: SIAM, 1990, 0-89871-360-9.

[20] B. Gustavsen and O. Mo, "Interfacing convolution based linear models to an electromagnetic transients program," presented at the Int. Conf. Power System Transients, Lyon, France, Jun. 4–7, 2007.

Bjørn Gustavsen (M'94–SM'03) was born in Harstad, Norway, in 1965. He received the M.Sc. and Dr.Ing. degrees from the Norwegian Institute of Technology (NTH), Trondheim, Norway, in 1989 and 1993, respectively.

Currently, he is with SINTEF Energy Research, Trondheim, where he has been since 1994. His interests include the simulation of electromagnetic transients and modeling of frequency-dependent effects. He was a Visiting Researcher at the University of Toronto, Toronto, ON, Canada, in 1996 and the Manitoba HVDC Research Centre, Winnipeg, MB, Canada, in 1998.

Dr. Gustavsen was a Marie Curie Fellow at the University of Stuttgart, Stuttgart, Germany, from 2001 to 2002.

John Nordstrom was born in Ottawa, ON, Canada, in 1970. He received the B.Eng. degree in electrical engineering from Lakehead University, Thunder Bay, ON, Canada, in 1997 and the M.Sc. degree from the University of Manitoba, Winnipeg, MB, Canada, in 2004.

Since 1998, he has been a Developer of the PSCAD simulation software—specifically the transmission lines and load-flow solution engines with the Manitoba HVDC Research Centre, Inc.